NSTC 國家科學及技術委員會
National Science and Technology Council
The cost of publication in *Journal of Biomedical Science* is borne
by the National Science and Technology Council (NSTC), Taiwan.

Journal of Biomedical Science

RESEARCH

Open Access

Check for updates

Excess glucose alone depress young mesenchymal stromal/stem cell osteogenesis and mitochondria activity within hours/days via NAD$^+$/SIRT1 axis

B. Linju Yen[1*†], Li-Tzu Wang[2,3,4†], Hsiu-Huang Wang[1], Chin-Pao Hung[2], Pei-Ju Hsu[1], Chia-Chi Chang[1,5], Chien-Yu Liao[1], Huey-Kang Sytwu[6,7] and Men-Luh Yen[2*]

Abstract

Background The impact of global overconsumption of simple sugars on bone health, which peaks in adolescence/ early adulthood and correlates with osteoporosis (OP) and fracture risk decades, is unclear. Mesenchymal stromal/ stem cells (MSCs) are the progenitors of osteoblasts/bone-forming cells, and known to decrease their osteogenic differentiation capacity with age. Alarmingly, while there is correlative evidence that adolescents consuming greatest amounts of simple sugars have the lowest bone mass, there is no mechanistic understanding on the causality of this correlation.

Methods Bioinformatics analyses for energetics pathways involved during MSC differentiation using human cell information was performed. In vitro dissection of normal versus high glucose (HG) conditions on osteo-/adipo-line-age commitment and mitochondrial function was assessed using multi-sources of non-senescent human and murine MSCs; for in vivo validation, young mice was fed normal or HG-added water with subsequent analyses of bone mar-row CD45$^-$ MSCs.

Results Bioinformatics analyses revealed mitochondrial and glucose-related metabolic pathways as integral to MSC osteo-/adipo-lineage commitment. Functionally, in vitro HG alone without differentiation induction decreased both MSC mitochondrial activity and osteogenesis while enhancing adipogenesis by 8 h' time due to depletion of nic-otinamide adenine dinucleotide (NAD$^+$), a vital mitochondrial co-enzyme and co-factor to Sirtuin (SIRT) 1, a longevity gene also involved in osteogenesis. In vivo, HG intake in young mice depleted MSC NAD$^+$, with oral NAD$^+$ precursor supplementation rapidly reversing both mitochondrial decline and osteo-/adipo-commitment in a SIRT1-dependent fashion within 1~5 days.

Conclusions We found a surprisingly rapid impact of excessive glucose, a single dietary factor, on MSC SIRT1 function and osteogenesis in youthful settings, and the crucial role of NAD$^+$—a single molecule—on both MSC

---

†B. Linju Yen and Li-Tzu Wang contributed equally to this work.

*Correspondence:
B. Linju Yen
blyen@nhri.edu.tw
Men-Luh Yen
mlyen@ntu.edu.tw
Full list of author information is available at the end of the article

BMC

Yen *et al. Journal of Biomedical Science*   (2024) 31:49

Page 2 of 17

mitochondrial function and lineage commitment. These findings have strong implications on future global OP and disability risks in light of current worldwide overconsumption of simple sugars.

Keywords Human mesenchymal stromal/stem cells (MSCs), Osteogenesis, Adipogenesis, Mitochondria, High glucose, Mouse model, Nicotinamide adenine dinucleotide (NAD$^+$), Nicotinamide mononucleotide (NMN), Sirtuin 1 (SIRT1)

Introduction

Excessive simple sugar/monosaccharide consumption is a global concern by strongly increasing numerous disease risks [1–7] but surprisingly its association with bone health and osteoporosis (OP), an age-related disease of bone fragility with outsized contributions to global disease disability by increasing fracture risks [8–10], has remained largely unclear. The cell responsible for bone formation is the osteoblast, a descendant cell type of the multilineage mesenchymal stromal/stem cell (MSC)—first identified in the non-hematopoietic/CD45$^-$ compartment of the bone marrow—which can also differentiate into other skeletal-related lineages particularly adipocytes and chondrocytes [11, 12]. MSC osteogenesis appears to be fragile, with senescence decreasing its osteogenic capacity but increasing adipogenic capacity [13–18]. The rapid aging of populations worldwide has made OP a critical public health concern, and despite the availability of numerous treatments and recent discoveries of potent biologics, patient compliance remains problematic due to slow improvement coupled with rare but severe adverse effects in all classes of therapeutics [19]. Unlike most tissues/organs, over 90% of peak bone mass is acquired by the age of 20, decades before the onset of OP and fracture risk, with bone loss beginning after the age of 30 [20–22]. Moreover during this time period, suboptimal lifestyle choices—one of few modifiable OP risk factors—including poor dietary habits strongly increase OP and fracture risks later in life [23]. Alarmingly, there are worrisome trends of plateauing height growth and low bone mass in ever younger people, with correlative evidence showing adolescents consuming the greatest amounts of simple sugars having the lowest bone mass [24–26]. Despite global sugar overconsumption and the widening epidemic of OP, molecular understanding of how excessive simple sugar/monosaccharide intake affects MSC osteogenic lineage commitment in youthful, non-senescent settings remains largely unexplored, with the existing few mechanistic studies yielding inconsistent results [27–30].

Found in all living cells, a vital co-enzyme involved in mitochondrial function is nicotinamide adenine dinucleotide (NAD$^+$) [31]. Intake of excessive or high glucose (HG), the most common monosaccharide, triggers glycolysis which depletes NAD$^+$ levels by requiring NAD$^+$ to accept electrons and form NADH. Under normal glucose conditions, however, mitochondrial function is maintained which improves NAD$^+$ levels and also the function of Sirtuin (SIRT) 1 [32], an NAD$^+$-dependent histone deacetylase with crucial roles in organismal longevity [33, 34] and MSC osteogenesis [35, 36]. While it is well known that aging and senescence decreases NAD$^+$ levels and bone mass [37, 38], the more relevant questions for bone health which anabolically peaks in adolescence/early adulthood, has surprisingly not been answered: whether modulating NAD$^+$ levels in young/non-senescent settings would impact MSC osteogenesis, and the role of simple sugar overconsumption on osteogenic commitment in young/non-senescent MSCs. We therefore investigated the role and any underlying mechanism of HG intake in modulating MSC mitochondrial function and lineage commitment in in vitro human and murine MSCs and in vivo. Our findings demonstrate surprisingly that HG intake alone can rapidly—within hours in vitro and 1–5 days in vivo—deplete NAD$^+$ levels, decreasing mitochondrial function and switching MSC lineage commitment from osteogenesis to adipogenesis by decreasing downstream SIRT1 actions. The findings not only demonstrate the detrimental and unexpected rapid impact of HG intake alone simultaneously on MSC mitochondrial function and osteogenic commitment in non-senescent settings, but also show the implications of simple sugar overconsumption on bone health even in youthful settings.

Methods

Cell culture and differentiation

Human bone marrow (BM) MSCs were obtained from commercial sources (Promocell, Heidelberg, Germany), while mouse BMMSCs were isolated from C57BL/6 J strain (National Laboratory Animal Center, Taipei, Taiwan). Human placental MSCs (PMSCs) were isolated as previously reported from term placental tissue (38–40 weeks' gestation) obtained from healthy donor mothers after informed consent approval [39]. All human MSCs were cultured in low-glucose Dulbecco's Modified Eagle's medium (DMEM) (Invitrogen -Thermo Fisher Scientific) with 10% FBS (Hyclone-Thermo Fisher Scientific), 100U/ml of penicillin/streptomycin, 2 mM L-glutamine (all from Gibco-Thermo Fisher Scientific)

Yen *et al. Journal of Biomedical Science*   (2024) 31:49

Page 3 of 17

[40]. Non-senescent MSCs, including passages 8–10 for BMMSCs and passages 15–20 for PMSCs, were used as previously reported [15, 41, 42]. Mouse C3H10T1/2 MSCs were obtained from American Type Culture Collection (ATCC, Manassas, VA, USA) and maintained in Basal Medium Eagle medium (BMEM) (Invitrogen-Thermo Fisher) with 10% FBS, 100 U/ml of penicillin/streptomycin, 2 mM L-glutamine [43]. Adipogenic and osteogenic differentiation with quantification of Oil Red O and Alizarin Red staining, respectively, were performed as previously reported [15, 39].

Bioinformatic analyses

Transcriptomic profiling databases were obtained from the National Center for Biotechnology Information-Gene Expression Omnibus database for bioinformatic analyses: GSE20631 for human BMMSCs, GSE45169 for human adipocytes, GSE101140 for human osteoblasts, and GSE128423 for single-cell RNA sequencing of uncultured BM CD45⁻ osteolineage cells and MSCs harvested from male C57BL/6 mice at age 6–8 weeks [44]. Principal component analysis (PCA) of transcriptomic profiles was performed using Partek® Flow® software (Partek, Inc., St. Louis, MO), while enriched pathways in Gene Ontology (GO) Biological Processes were performed using Gene set enrichment analysis (GSEA) which showed positive enrichment with a normalized enrichment score (NES) > 1 and a p-value < 0.05, as well as Metascape analysis in which significance was set at p-value < 0.01 [45]. The Molecular Activation Prediction (MAP) tool was used to interrogate networks and pathways with expression levels of involved genes using Ingenuity Systems Pathway Analysis (IPA) software (QIAGEN, Hilden, Germany) [46]. IPA showed regulatory relationships between up-regulatory (red) and down-regulatory (green) molecules, while the MAP tool predicted that the targeted processes or involved molecules were activated (orange) or inhibited (blue) through relationships with positive regulation (orange lines), negative regulation (blue lines), inconsistent findings (yellow lines), or being not predicted (gray lines). Dashed lines represented indirect interactions based on published data.

Real-time PCR

RNA was extracted with TRIzol reagent (Invitrogen-Thermo Fisher Scientific) and cDNA synthesis was performed with ReverTra Ace set (TOYOBO, Osaka, JP), both according to the manufacturer's protocols. SYBR was applied for the assessment of PCR products by ABI 7500 Fast Real-Time PCR system (Thermo Fisher Scientific). Primers for human and murine genes are listed in Table 1.

Table 1 The list of primer sequence for qPCR

Gene		Forward primer	Reverse primer
Human	*GAPDH* (internal control)	5'-GTGGACCTGACCTGCCGTCT-3'	5'-GGAGGAGTGGGTGTCGCTGT-3'
	GLUT1	5'-CATCAACCGCAACGAGGAGAAC-3'	5'-CAGCACCACAGCGATGAGGAT-3'
	GLUT2	5'-GCTGCCGCTGAGAAGATTAGAC-3'	5'-CCTGACTAGCTCCTGCCTGTT-3'
	GLUT3	5'-ACGGCCTCATGGAGAATGAACAG-3'	5'-AGCAGCATTCAGAAGCGTCCT-3'
	GLUT4	5'-ATCCTTGGACGATTCCTCATTGG-3'	5'-CAGGTGAGTGGGAGCAATCT-3'
	ADIPOQ	5'-GCTCAGCATTCAGTGTGGGA-3'	5'-GTACAGCCCAGGAATGTTGC-3'
	IBSP	5'-GGCCACGATATTATCTTTACAAGCA-3'	5'-CCTCAGAGTCTTCATCTTCA-3'
	CEBPB	5'-AAACTCTCTGCTTCTCCCTCTG-3'	5'-GTTGCGTCAGTCCCGTGTA-3'
	KLF5	5'-CCTGGTCCAGACAAGATGTGA-3'	5'-GAACTGGTCTACGACTGAGGC-3'
	RUNX2	5'-CCAGATGGGACTGTGGTTACTG-3'	5'-TTCCGGAGCTCAGCAGAATAA-3'
	ALPL	5'-AGCTGAACAGGAACAACGTGA-3'	5'-CTTCATGGTGCCCGTGGTC-3'
Murine	*Actb* (internal control)	5'-GAAATCGTGCGTGACATCAAAG-3'	5'-TGTAGTTTCATGGATGCCACAG-3'
	Glut1	5'-GGTGCCAGCCAAAGTGACAAC-3'	5'-GTCGGTTCGGAAGAGGTCTCAT-3'
	Glut2	5'-TTCCAGTTCGGCTATGACATCG-3'	5'-CTGGTGTGACTGTAAGTGGGG-3'
	Glut3	5'-CGGTGTGGAGTTGAACAGCAT-3'	5'-ATAGCAGCACTCAGAAGCAGTC-3'
	Glut4	5'-AGCCAGCCTACGCCACCATA-3'	5'-CTGGTGTGACTGTAAGTGGGG-3'
	Adipoq	5'-TGTTCCTCTTAATCCTGCCCA-3'	5'-CCAACCTGCACAAGTTCCCTT-3'
	Ibsp	5'-TAGTTCCGAAGAGGAGGGGG-3'	5'-CCCTGCTTTCTGCATCTCCA-3'
	Cebpb	5'-ACAAGCTGAGAGACGAGTACAAGA-3'	5'-GCAGCTGCTTGAACAAGTTCCG-3'
	Klf5	5'-AGGACTCATACGGGCGAGAA-3'	5'-ATGCACTGGAACGGCTTGG-3'
	Runx2	5'-GGT TAA TCT CCG CAG GTC ACT-3'	5'-CAC TGT GCT GAA GAG GCT GTT-3'
	Alpl	5'-CTGACTGACCCTTCGCTCTC-3'	5'-TGCTTGGCCTTACCCTCAT-3'

Yen *et al. Journal of Biomedical Science*   (2024) 31:49

Page 4 of 17

Mitochondrial activity assays

Mitochondrial activity was determined by the assessment of OCR using Seahorse XFe24 Analyzer (Agilent Technologies, Santa Clara, CA, USA) as previously reported [47] and mitochondrial ΔΨm. with JC-1 (Thermo Fisher Scientific) staining according to the manufacturer's protocol. For OCR assay, 2×10^4 MSCs were seeded in a 24XF cell culture microplate, cultured for 8 h, and then replaced with Seahorse XF DMEM media in which contain 2% FBS, 2 mM glutamine and 1 g/L glucose with a 7.4 pH and incubated at 37 °C for extra 30 min. OCR was determined with a sequential treatment of 1 μM oligomycin, 2 μM carbonyl cyanide-p-trifluoromethoxyphenylhydrazone (FCCP) and rotenone combined with antimycin A during the analysis process. For mitochondrial ΔΨm. assay, 2×10^5 MSCs were treated with 2.5 μM JC-1 and then incubated at 7 °C for 30 min. Fluorescence signals were captured by fluorescence microscopy or quantified by flow cytometry. Depolarized mitochondrial ΔΨm. was assessed by detecting green fluorescence signals while polarized mitochondrial ΔΨm. was assessed by detecting red fluorescence signals. Gating for fluorescent signals of green$^+$/red$^-$, green$^+$/red$^+$ and green$^-$/red$^+$ was also performed for frequency analyses of low, intermediate and high mitochondrial ΔΨm., respectively.

Nicotinamide adenine dinucleotide (NAD$^+$)/NADH assay

The ratio of cellular NAD$^+$/NADH was assessed with colorimetric assay according to the manufacturer's protocol (Abcam, Cambridge, UK). Briefly, NADH amount was first measured by heating at 60°C for 30 min to decompose NAD$^+$ with developer reaction for measurement at OD 450 nm, and then convert NAD$^+$ to NADH for measurement of total NAD$^+$ and NADH (NADt). NAD+/NADH ratio can be calculated by the formula: (NADt-NADH)/NADH.

SIRT1 protein detection

Human BMMSCs were cultured in specific conditions for 8 h, with subsequent extraction of total cellular protein for assessment of SIRT1 expression with β-actin as an internal control by western blot analyses (all antibodies from Santa Cruz, CA, USA).

In vivo mouse experimentation

Animal experimentation was conducted following approved protocols by the Institutional Animal Care and Use Committee of the National Taiwan University (No. 20170426). 6-week-old C57BL/6 male mice were given drinking water with added glucose prepared by adding 13 g D-glucose (Sigma) into 100 ml drinking water [48] for 1 day or 5 days. Nicotinamide mononucleotide (NMN) was also orally provided in drinking water with a concentration of 2 g/L [49], and sirtinol was intraperitoneally administered with a dose of 1 mg/kg/day [50]. Mice were euthanized on day 1 or day 5, with uncultured CD45- BM cells harvested for RNA extraction and assessment of gene expression as well as JC-1 staining for assessment of mitochondrial function.

Statistical analysis

For comparisons between two groups, Student's *t*-test was used, while for comparisons between multiple groups, ANOVA was used followed by Tukey test. A value of $p < 0.05$ was considered statistically significant. Analyses were performed using GraphPad Prism software (CA, USA) and data are shown as mean ± SD.

Results

Glucose-related metabolic pathways and mitochondria activity are integral to MSC lineage commitment, with HG alone without additional lineage induction able to shift human & murine MSCs to favor adipogenesis at the expense of osteogenesis

To assess the involvement of various energetic pathways in MSC lineage commitment towards adipogenesis or osteogenesis, we first performed PCA analysis of whole transcriptomic profiling of human BMMSCs, adipocytes and osteoblasts to ascertain that the 3 cell types have distinctive profiles (Fig. 1A). Bioinformatics analyses revealed a number of carbohydrate- and glycolysis-related metabolic pathways to be significantly enriched in adipocytes vs. BMMSCs, while mitochondria-related and glucose homeostasis pathways were significantly enriched in osteoblasts vs. BMMSC (Fig. 1B). GSEA also supported the importance of glucose-related processes in adipocytes but not osteoblasts vs. BMMSCs by significantly upregulating "Positive regulation of glucose import" pathway (Fig. 1C) and "Regulation of glucose metabolic process" (Fig. 1D). In addition, we used the MAP tool from IPA and found that the process of "Glycolysis" was upregulated in adipocytes but downregulated in osteoblasts when compared to BMMSCs (Fig. 1E), suggesting that this process is more critically involved in adipogenesis rather than osteogenesis. To determine whether changes in glucose levels could functionally affect MSC lineage commitment to adipogenesis or osteogenesis, we first assessed the gene expression of glucose transporters in both human and murine MSCs of two tissue sources. We found that expression levels of insulin-independent *GLUT1*/*Glut1* and *GLUT3*/*Glut3* were significantly higher than insulin-dependent *GLUT2*/*Glut2* and *GLUT4*/*Glut4* in primary human BMMSCs, human placental MSCs (PMSCs), and mouse BMMSCs regardless of treated glucose levels—either low glucose (LG; 5.5 mM) or HG (25 mM); similar findings were seen in the mouse C3H10T1/2 MSC line (C3H) which only
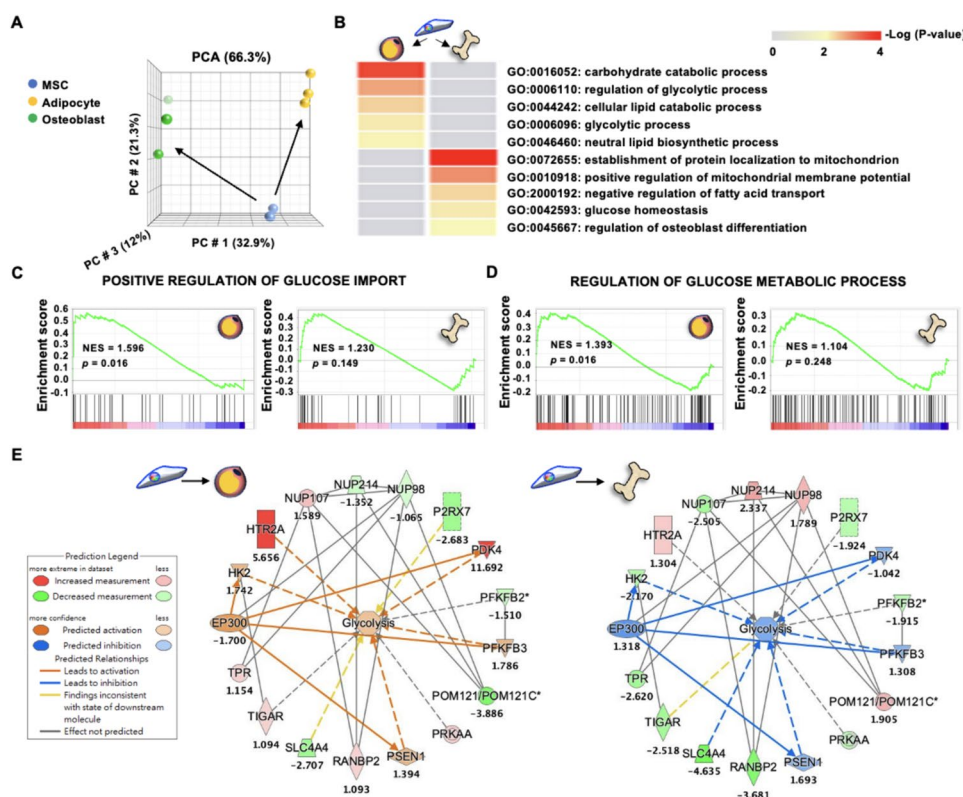
Fig. 1 Mitochondrial and glucose homeostasis pathways were highly associated with osteogenesis, while glycolysis-related pathways were highly associated with adipogenesis. **A** Principal component analysis (PCA) of transcriptomic profiles of human bone marrow (BM) mesenchymal stem cells (MSCs; *n* = 3, GSE20631), adipocytes (*n* = 3, GSE45169), and osteoblasts (*n* = 3, GSE101140). **B** Metascape pathway analyses for enriched GO Biological Processes in adipocytes and osteoblasts compared to BMMSCs using transcriptomic data, with pathways colored according to *p* values. **C** Enrichment of "Positive regulation of glucose import" pathway as performed by Gene set enrichment analysis (GSEA) in adipocytes or osteoblasts compared to BMMSCs, with normalized enrichment score (NES) and *p* value labeled. **D** Enrichment of "Regulation of glucose metabolic process" pathway as performed by GSEA in adipocytes and osteoblasts compared to BMMSCs, with NES and *p* value labeled. **E** Prediction of mechanisms involved in "Glycolysis" as performed with the Molecular Activation Prediction (MAP) tool using transcriptomic data from adipocytes or osteoblasts compared to BMMSCs

expressed the insulin-independent *Glut1* (Figure S1). These data suggest that glucose uptake in MSCs is generally insulin-independent. In vitro functional assessment of adipogenesis was significantly increased in primary human and murine MSCs cultured in adipogenic medium (AM) containing HG compared to LG, as evidenced by Oil Red (OR) staining for oil droplets (Fig. 2A, B). However, osteogenic capacity of all three primary MSCs was significantly decreased in osteogenic medium (OM) with HG compared to LG, as assessed by Alizarin Red (AR) staining for calcium deposition (Figs. 2C, D). More surprisingly, even when MSCs were cultured in just control/expansion medium (CM) without any differentiation induction, addition of HG (HG-CM) increased expression levels of adiponectin (*ADIPQ*/*Adipoq*), an adipocyte lineage gene, in human BMMSCs and PMSCs as well as mouse BMMSCs and C3H, while simultaneously decreasing levels of bone sialoprotein (*IBSP*/*Ibsp*),

an osteogenic lineage gene, in all four MSCs (Fig. 2E-H), suggesting a potential role for HG alone in driving MSC lineage specification towards adipogenesis over osteogenesis even without overt induction by lineage-specific differentiation medium. Collectively, these results suggest that HG alone can trigger lineage commitment of MSCs towards adipogenesis and away from osteogenesis.

HG alone decreased mitochondrial activity and triggered MSC adipogenesis over osteogenesis within 8 h due to depletion of NAD+

To further elucidate the mechanisms involved in triggering of MSC adipogenic over osteogenic commitment by HG alone, we first assessed the earliest time point at which the adipogenic and osteogenic master transcription factors CCAAT/enhancer-binding protein beta *(Cebpb)* and Runt-related transcription factor 2 (*Runx2*), respectively, are upregulated during differentiation into

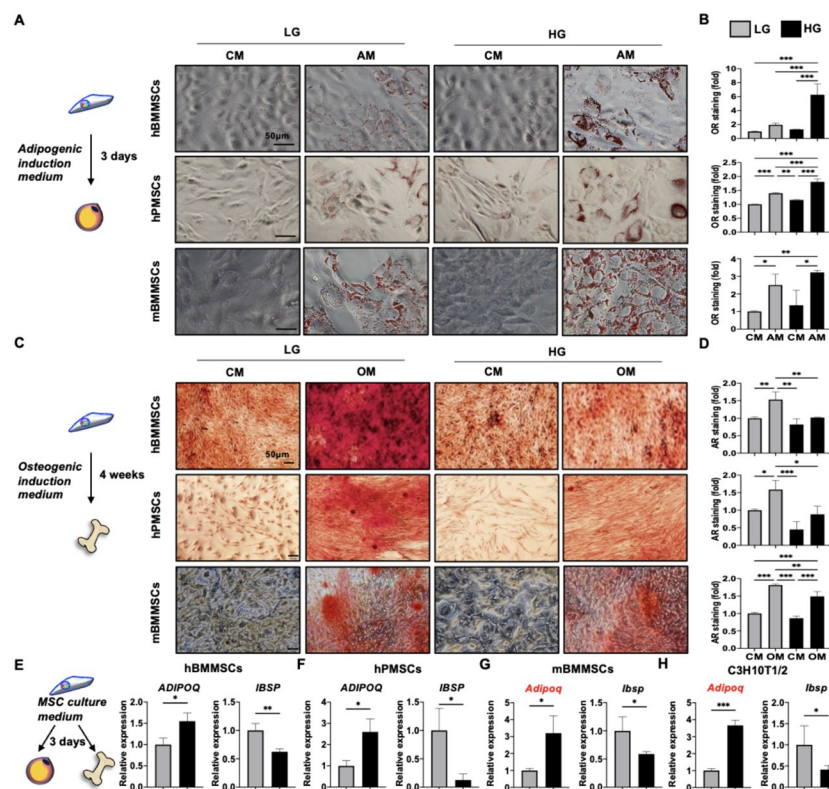Yen *et al. Journal of Biomedical Science*   (2024) 31:49

Page 6 of 17

Fig. 2 High glucose (HG) alone can commit human and murine MSCs towards adipogenesis while inhibiting osteogenesis. **A** and **B** Representative data and pooled data of lipid droplet accumulation as assessed in human BMMSCs (top panel), human placental MSCs (PMSCs; middle panel), or murine BMMSCs (bottom panel) by staining with Oil Red (OR). Scale bar, 50 μm. **C** and **D** Representative and pooled data of extracellular mineralization as assessed in human BMMSCs (top panel), human PMSCs (middle panel), or murine BMMSCs (bottom panel) by staining with Alizarin Red (AR). Scale bar, 50 μm. **E** and **F** qPCR analyses of functionally adipogenic and osteogenic genes, adiponectin (*ADIPOQ*) and bone sialoprotein (*IBSP*), in human BMMSCs (**E**) and PMSCs (**F**), treated with LG or HG for 3 days. **G** and **H** qPCR analyses of *Adipoq* and *Ibsp* in murine BMMSCs (**G**) and mouse C3H10T1/2 mesenchymal progenitor/stem cells (C3H; **H**), treated with LG or HG for 3 days. $N = 3$ for each group in all figures. Data are shown as mean ± SD. *, $p < 0.05$; **, $p < 0.01$; ***, $p < 0.001$

the respective lineages. To our surprise, we found that each master lineage transcription factor was rapidly induced in the respective media at just 8 h (Fig. 3A). To explore whether HG alone without differentiation induction could influence MSC lineage commitment also at this early time point, we profiled the 2 master transcription factors as well as 2 early markers for each lineage—Kruppel-like factor 5 (*Klf5*) for adipogenesis and alkaline phosphatase (*Alpl*) for osteogenesis—in C3H cultured in CM only with HG added. We found that expression levels of both *Cebpb* and *Klf5* were significantly upregulated in C3H with HG-CM at this early time point (Fig. 3B); conversely, expression of *Runx2* and *Alpl* were significantly downregulated at this time point in these same conditions (Fig. 3C). With the crucial role of NAD$^+$ in metabolism, mitochondrial activity, as well as MSC osteogenesis via the NAD$^+$-dependent deacetylase SIRT1, we assessed whether HG altered cellular levels of NAD$^+$ and found that C3H cultured in HG-CM had a significantly decreased ratio of NAD$^+$/

NADH compared to cells cultured in standard LG-CM at 8 h (Fig. 3D). Bioinformatics analyses using the MAP tool predicted downregulation in the process of "Function of mitochondria" during MSC differentiation towards adipocytes but upregulation during differentiation towards osteoblasts (Fig. 3E). To confirm this prediction, we assessed the oxidative phosphorylation (OXPHOS) pathway using the Seahorse assay which revealed that MSCs cultured in HG demonstrated a significantly decreased maximal oxygen consumption rate (OCR; Fig. 3F, G, which suggests that the mitochondrial membrane potential (ΔΨm.)—an important parameter of mitochondrial function—was impaired by HG. To further validate these findings, we stained C3H cultured in HG-CM with a mitochondrial ΔΨm.-sensitive dye JC-1 and found at 8 h, these cells lost membrane potential compared to C3H cultured in LG-CM: similar intensity of green fluorescence representing depolarized mitochondrial ΔΨm. between LG- and HG-treated cells could be seen, but significantly lower intensity of red fluorescence

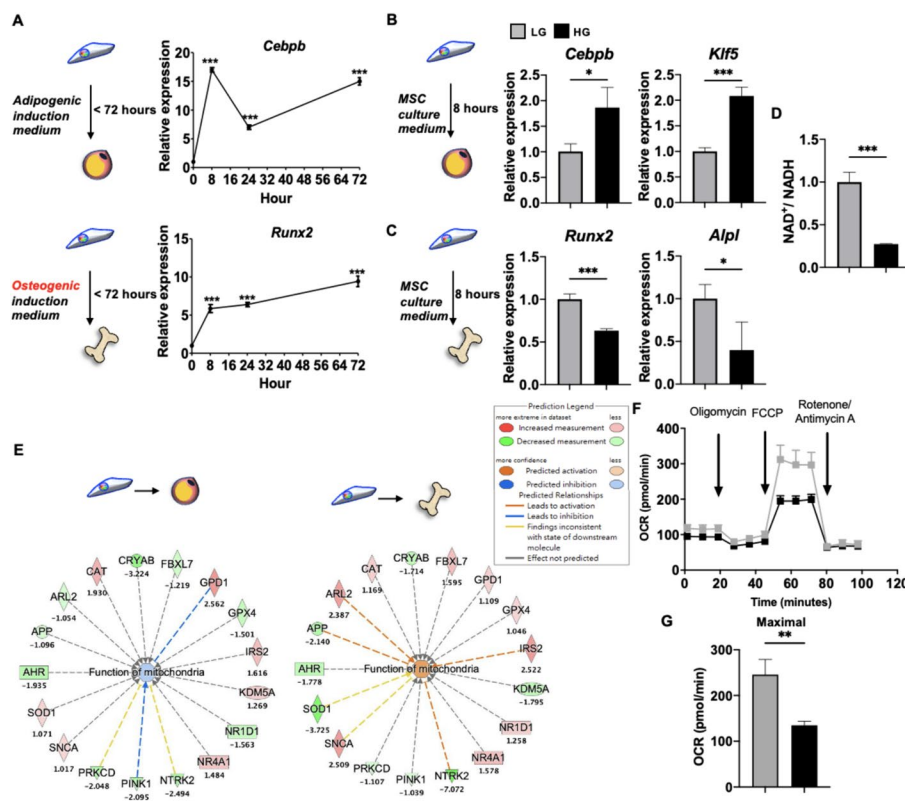Yen *et al. Journal of Biomedical Science* (2024) 31:49

Page 7 of 17

Fig. 3 HG alone can trigger MSC adipogenesis over osteogenesis with depletion of nicotinamide adenine dinucleotide (NAD$^+$) and depression of mitochondrial activity by 8 h. **A** qPCR analyses of early adipogenic and osteogenic genes, CCAAT/enhancer-binding protein beta (*Cebpb*) and Runt-related transcription factor (*Runx2*) as assessed in C3H with AM and OM, respectively. **B** qPCR analyses of early adipogenic genes, *Cebpb* and Kruppel-like factor 5 (*Klf5*) as assessed in C3H cells with CM containing LG or HG for 8 h. **C** qPCR analyses of early osteogenic genes, *Runx2* and alkaline phosphatase (*Alpl*) as assessed in C3H cells with CM containing LG or HG for 8 h. **D** Ratio of cellular NAD$^+$ to NADH (NAD.$^+$/NADH) as assessed in C3H with CM containing LG or HG for 8 h ($n = 4$ for each group). **E** MAP prediction of mechanisms involved in "Function of mitochondria" using transcriptomic data from human adipocytes ($n = 3$, GSE45169) or osteoblasts ($n = 3$, GSE101140) compared to BMMSCs ($n = 3$, GSE20631). **F** Oxygen consumption rates (OCRs) of C3H cultured in LG or HG conditions for 8 h as assessed by Seahorse assay. **G** Quantification of maximal OCRs in LG- or HG-cultured C3H. $N = 3$ for each group in all figures except D. Data are shown as mean ± SD. *, $p < 0.05$; **, $p < 0.01$; ***, $p < 0.001$

representing polarized mitochondrial ΔΨm. was seen in HG- vs. LG-treated cells (Fig. 4A, B). To globally visualize the changes in mitochondrial ΔΨm. brought by HG, we performed t-distributed stochastic neighbor embedding (t-SNE) analyses and found that both intermediate and high ΔΨm. were more prominent in LG-treated cells than HG-treated cells (Fig. 4C). Verification with flow cytometry analyses (Fig. 4D-F) also demonstrated that HG similarly decreased the intensity of polarized mitochondrial ΔΨm.; further analyses also showed that HG significantly decreased mitochondria with intermediate ΔΨm. (represented by double positivity for red and green fluorescence), while increasing mitochondria with low ΔΨm. (green fluorescence positivity only) and decreasing mitochondria with high ΔΨm. (red fluorescence positivity only) albeit non-significantly.

To explore whether NAD$^+$-mediated mitochondrial function is involved in regulating MSC lineage commitment, we inhibited NAD$^+$ biosynthesis with FK866 (FK) in LG-CM-cultured C3H and at 8 h, and found that both the intensity of polarized mitochondrial ΔΨm. (Fig. 4G) as well as the frequency of mitochondria with either intermediate or high ΔΨm. were significantly decreased; the frequency of mitochondria with low ΔΨm. was significantly increased (Fig. 4H). Furthermore, analyses of lineage gene expression in FK-treated C3H demonstrated a shift from osteogenesis to adipogenesis, as evident by significant upregulation of *Cebpb* and *Klf5* with concomitant downregulation of *Runx2* and *Alpl* (Fig. 4I, J). Conversely, supplementation with nicotinamide mononucleotide (NMN), a precursor of NAD$^+$ [31, 51], to C3H cultured in HG-CM resulted in an increase in NAD$^+$ levels in just 8 h which reversed mitochondrial ΔΨm. and the frequencies of mitochondria with intermediate and high ΔΨm. (Fig. 4K, L); moreover, lineage commitment was shifted back to osteogenesis and away from adipogenesis as evidenced by significant downregulation of
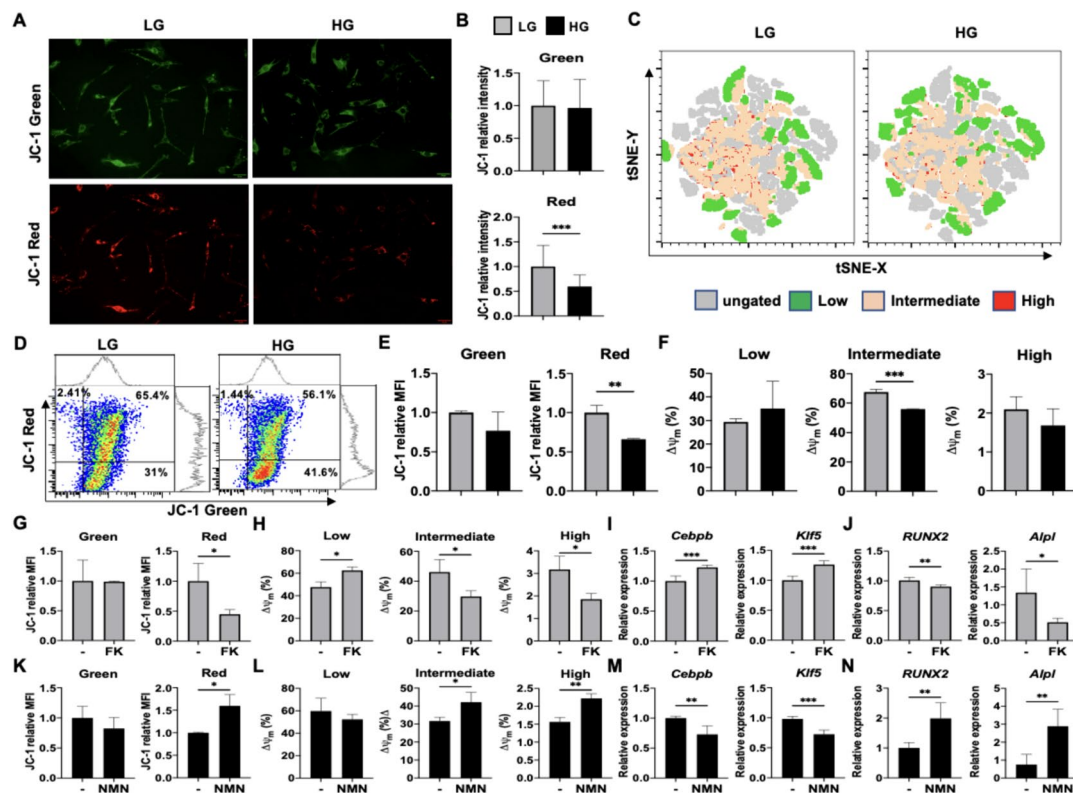
Yen *et al. Journal of Biomedical Science*   (2024) 31:49

Page 8 of 17

Fig. 4 HG alone depress MSC osteogenesis and mitochondrial activity while enhancing adipogenesis, which are all reversed with nicotinamide mononucleotide (NMN) supplementation. **A** Representative data for mitochondrial activity of C3H as assessed with JC-1 staining by fluorescence microscopy at hour 8. Scale bar, 50 μm. **B** Pooled data for depolarized and polarized mitochondrial membrane potential (ΔΨm.) in C3H, as assessed by measuring fluorescence signals with Image J (three photos for each group with a total of 81 cells for LG and 83 cells for HG). **C** Population analyses for low, intermediate and high mitochondrial activity with PhenoGraft on the t-distributed stochastic neighbor embedding (t-SNE) map. C3H cells were cultured with LG or HG for 8 h, and then stained with JC-1, followed by flow cytometric analysis with t-SNE-based algorithm. **D** Representative data for frequency analyses of low, intermediate and high mitochondrial activity as assessed in C3H with CM containing LG or HG by flow cytometry at hour 8. **E** Pooled data of depolarized and polarized mitochondrial ΔΨm. as assessed in C3H with CM containing LG or HG by analyzing green intensity and red intensity, respectively. **F** Pooled data for frequency analyses of low, intermediate and high mitochondrial activity as assessed in C3H with CM containing LG or HG. **G** Pooled data of depolarized and polarized mitochondrial ΔΨm. as assessed in C3H with LG-CM in the absence or presence of FK866 (FK; 5 nM). **H** Pooled data for frequency analyses of low, intermediate and high mitochondrial activity as assessed in C3H with LG-CM in the absence or presence of FK. **I** and **J** qPCR analyses of *Cebpb* and *Klf5* (**I**) as well as *Runx2* and *Alpl* (**J**) as assessed in C3H with LG-CM in the absence or presence of FK. **K** Pooled data of depolarized and polarized mitochondrial ΔΨm. as assessed in C3H with HG-CM in the absence or presence of NMN (50 μM). **L** Pooled data for frequency analyses of low, intermediate and high mitochondrial activity as assessed in C3H with HG-CM in the absence or presence of NMN. (M and N) qPCR analyses of *Cebpb* and *Klf5* (**M**) as well as *Runx2* and *Alpl* (**N**) as assessed in C3H with HG-CM in the absence or presence of NMN. $N = 3$ for each group in all figures except B. Data are shown as mean ± SD. *, $p < 0.05$; **, $p < 0.01$; ***, $p < 0.001$

Cebpb and *Klf5* with significant upregulation of *Runx2* and *Alpl* simultaneously (Fig. 4M, N). To further confirm the role of NAD$^+$-mediated mitochondrial metabolism in MSC lineage commitment, we cultured C3H in CM containing galactose (Gal) which diverts cells from glycolysis to mitochondrial metabolism thereby rapidly increasing cellular NAD$^+$ within a few hours (Figure S2A) [52]. Mitochondrial parameters in Gal-CM-cultured C3H demonstrated significantly increased ΔΨm. (Figures S2B, C), with the frequency of mitochondria with low ΔΨm. significantly decreased

while frequency of mitochondria with intermediate ΔΨm. was significantly increased (Figure S2D). Treatment with Gal also shifted C3H lineage commitment towards osteogenesis, with significant downregulation of *Cebpb* and *Klf5* alongside significant upregulation of *Runx2* and *Alpl* at 8 h' time (Figures S2E-F). HG in vitro conditions have long been known to promote oxidative stress in numerous cell types [53–55], therefore to evaluate whether oxidative stress was involved in this rapid lineage commitment shift in MSCs, we assessed levels of reactive oxidative species (ROS) in LG

Yen *et al. Journal of Biomedical Science* (2024) 31:49

Page 9 of 17

vs. HG-treated MSCs. We found that ROS levels were similar in LG- and HG-treated MSCs up until 24 h of time and not significantly changed until 48 h after (Figure S2G, H), which is much later than the depletion of NAD$^+$ with HG at 8 h. Collectively, these findings demonstrate that HG conditions rapidly reduce cellular NAD$^+$ levels, leading to diminished mitochondrial function and a shift in MSC lineage commitment from adipogenesis to osteogenesis within 8 h. These consequences of HG can be reversed by supplementation with NMN/NAD$^+$ or inhibition of NAD$^+$ depletion.

HG alone rapidly downregulates SIRT1 expression and functions to suppress mitochondrial activity as well as MSC osteogenesis via NAD$^+$ depletion

SIRT1 activity is NAD$^+$-dependent, which uniquely confers a dual role for this molecule in MSCs: modulating mitochondrial function as well as osteogenic lineage commitment [56]. Surprisingly, however, understanding of how excess levels of simple sugars can affect these dual aspects of SIRT1's actions in MSCs remain unclear. To explore whether the NAD$^+$/SIRT1 axis is involved in HG-mediated MSC mitochondrial metabolic changes and adipogenic/osteogenic lineage commitment, we first assessed SIRT1 protein expression at 8 h and found that protein levels were significantly decreased in human BMMSCs cultured in HG-CM compared to cells cultured in LG-CM (Fig. 5A, B). Moreover, inhibition of NAD$^+$ biosynthesis with FK significantly decreased SIRT1 protein levels in LG-CM-cultured human BMMSCs, whereas NMN supplementation significantly increased SIRT1 levels in HG-CM-cultured cells. Higher NAD$^+$ levels have been shown to enhance SIRT1 expression in a number of studies [57, 58], and the mechanism appears to be mainly through protein stabilization including NAD$^+$-mediated
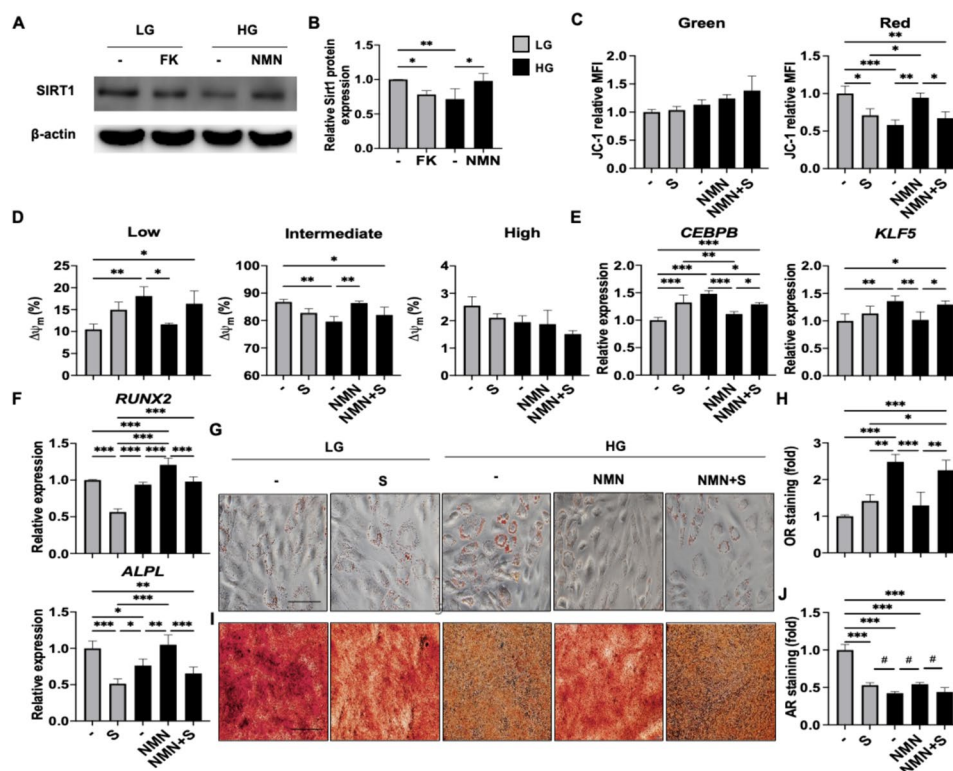

Fig. 5 HG alone rapidly downregulates Sirtuin (SIRT) 1 expression and function to suppresses mitochondrial activity as well as MSC osteogenesis via NAD$^+$ depletion. **A** & **B** Representative and pooled data for expression levels of SIRT1 protein in human BMMSCs cultured in LG-CM or HG-CM for 8 h as assessed by western blot, respectively ($n=4$ for each group). **C** Pooled data of depolarized and polarized mitochondrial ΔΨm. as assessed in human BMMSCs treated with LG-CM in the absence or presence of sirtinol (S; 20 μM), or HG-CM in the absence or presence of NMN or NMN combined with S for 8 h ($n=3$ for each group). **D** Pooled data for frequency analyses of low, intermediate and high mitochondrial activity as assessed in human BMMSCs treated with LG-CM in the absence or presence of S, or HG-CM in the absence or presence of NMN or NMN combined with S for 8 h ($n=3$ for each group). (E and F) qPCR analyses of *CEBPB* and *KLF5* (**E**) as well as *RUNX2* and *ALPL* (**F**) as assessed in human BMMSCs treated with LG-CM in the absence or presence of S, or HG-CM in the absence or presence of NMN or NMN combined with S for 8 h ($n=4$ for each group). **G** and **H** Representative and pooled data ($n=3$ for each group), respectively, for oil drop accumulation in human BMMSCs as assessed with OR staining. Scale bar, 50 μm. **I** and **J** Representative and pooled data ($n=3$ for each group), respectively, for calcium deposition in human BMMSCs as assessed with AR staining. Scale bar, 50 μm. Data are shown as mean ± SD. *, $p < 0.05$; **, $p < 0.01$; ***, $p < 0.001$. #, $p < 0.05$ for comparison excluding LG-OM (1.st bar)

Yen *et al. Journal of Biomedical Science*   (2024) 31:49

Page 10 of 17

downregulation of JNK phosphorylation [59, 60] which we also found to be true (Figure S3A-D).

To assess the role of SIRT1 in modulating MSC mitochondrial activity, we treated LG-CM-cultured human BMMSCs with the SIRT1 inhibitor sirtinol (S) for 8 h which significantly decreased polarized mitochondrial ΔΨm. to levels similar to HG-CM-cultured cells; this could be rescued with NMN supplementation but not if SIRT1 activity was blocked (Figs. 5C & S3E-F). Flow cytometric analyses also demonstrated that inhibition of SIRT activity in LG-CM-cultured human BMMSCs increased the frequency of mitochondria with low ΔΨm., which were significantly decreased in HG-CM-culture cells supplemented with NMN; further inhibition of SIRT1 activity reversed this effect (Figs. 5D & S3G). The inverse trend was seen for mitochondria with intermediate ΔΨm., in which SIRT1 inhibition in LG-CM-cultured human BMMSCs decreased frequencies; in cells cultured in HG-CM, frequencies of such mitochondria were significantly increased after NMN supplementation and decreased after simultaneous SIRT1 inhibition (Figs. 5D & S3H-I). At 8 h' time, adipogenic genes *CEBPB* and *KLF5* were upregulated whereas osteogenic genes *RUNX2* and *ALPL* were downregulated in LG-CM-cultured human BMMSCs, as well as cells cultured in HG-CM with NMN supplementation after SIRT1 inhibition (Figs. 5E-F & S3J-M). Functional differentiation assays validated the lineage-specific gene expression patterns (Figs. 5G-J & S3N-O): addition of HG to AM resulted in a doubling of oil droplet formation in human BMMSCs compared to LG-AM induction; conversely, HG-OM culture resulted in a more than 50% decrease in mineralization compared to LG-OM. Interestingly, SIRT1 inhibition in LG conditions increased oil droplet accumulation in AM-cultured human BMMSCs by over 40%, in OM-culture

cells a more severe reduction of extracellular mineralization by nearly half was seen, and while NMN supplementation in HG-AM significantly decreased oil droplet formation, simultaneous inhibition of SIRT1 abrogated this effect; the converse was seen in HG-OM cultured human BMMSCs, with NMN supplementation resulting in a significant increase of mineralization compared to baseline HG-OM levels, which was largely abrogated when SIRT1 was inhibited at the same time. Interestingly, increasing *SIRT1* at the level of gene expression can also achieve similar results (Figure S3P-T), underscoring the critical role of SIRT1 in MSC lineage commitment. These findings demonstrate that LG conditions promote MSC osteogenesis as well as mitochondrial function through upregulation of the NAD⁺/SIRT1 axis, while HG conditions promote MSC adipogenic commitment and decrease mitochondrial metabolism by downregulating this axis within 8 h.

In vivo HG intake rapidly downregulates mitochondrial activity and triggers adipogenic over osteogenic commitment in CD45⁻ BM cells that can be rapidly and strongly reversed with oral NMN supplementation in a SIRT1-dependent fashion

To investigate the translational relevance of the in vitro results of HG conditions on MSC mitochondrial metabolism and lineage commitment, we first performed bioinformatics analyses to assess relevant pathways in single-cell RNA transcriptomics of uncultured CD45⁻ BM osteolineage cells vs. MSCs harvested from young adult mice. We found that pathways involving bone formation and mitochondrial activities including ΔΨm. and ATP synthesis were enriched (Fig. 6A); moreover, treatment with high levels of glucose was predicted to downregulate mitochondrial functions via multiple transcription regulators including SIRT1 (Fig. 6B).

(See figure on next page.)

Fig. 6 In vivo HG intake rapidly downregulates mitochondrial activity and triggers adipogenic over osteogenic commitment in CD45⁻ BM cells that can be rapidly and strongly reversed with oral NMN supplementation in a SIRT1-dependent fashion. **A** Enrichment of bone- and mitochondria-related pathways as assessed in single-cell RNA transcriptomics of uncultured BM CD45⁻ osteolineage cells vs. MSCs harvested from young adult mice (NCBI-GEO database: GSE128423) using Metascape analysis. **B** Pathway analysis on the process of "function of mitochondria" involving transcription regulators with treatment of high levels of glucose as performed by MAP tool in IPA. The MAP tool showed that "function of mitochondria" is downregulated (blue) through positively regulated (orange line), negatively regulated (blue lines), and unpredicted (yellow line) downstream molecules after treatment of high levels of glucose (red). **C** Representative data for frequency analyses of low and intermediate mitochondrial activity as assessed in uncultured CD45⁻ BM cells of wildtype young adult C57BL/6 mice fed normal drinking water combined with intraperitoneal (i.p.) administration of S or not, or given drinking water with additional glucose with or without NMN, or NMN combined with i.p. injection of S. **D** Pooled data of depolarized and polarized mitochondrial ΔΨm. as assessed in CD45⁻ BM cells. **E** Pooled data for frequency analyses of low and intermediate mitochondrial activity as assessed in uncultured CD45⁻ BM cells. **F** and **G** qPCR analyses of *Cebpb* and *Klf5* (**F**) as well as *Runx2* and *Alpl* (**G**) in BM cells. $N = 3$ for each group in all figures. Data are shown as mean ± SD. *, $p < 0.05$; **, $p < 0.01$; ***, $p < 0.001$. **H** Heatmap plots as generated comparing relative expression levels of *CEBPB/Cebpb*, *KLF5/Klf5*, OR staining, *RUNX2/Runx2*, *ALPL/Alpl*, AR staining as well as in vitro and in vivo mitochondrial activities between LG and HG groups in vitro or H₂O and glucose groups in vivo. (I) Summary: HG intake for a few hours or days rapidly depresses mitochondrial activity and osteogenesis while strongly promoting adipogenesis via the NAD⁺/SIRT1 axis in non-senescent MSCs, with rescue of both mitochondrial activity and osteogenesis possible through NMN supplementation
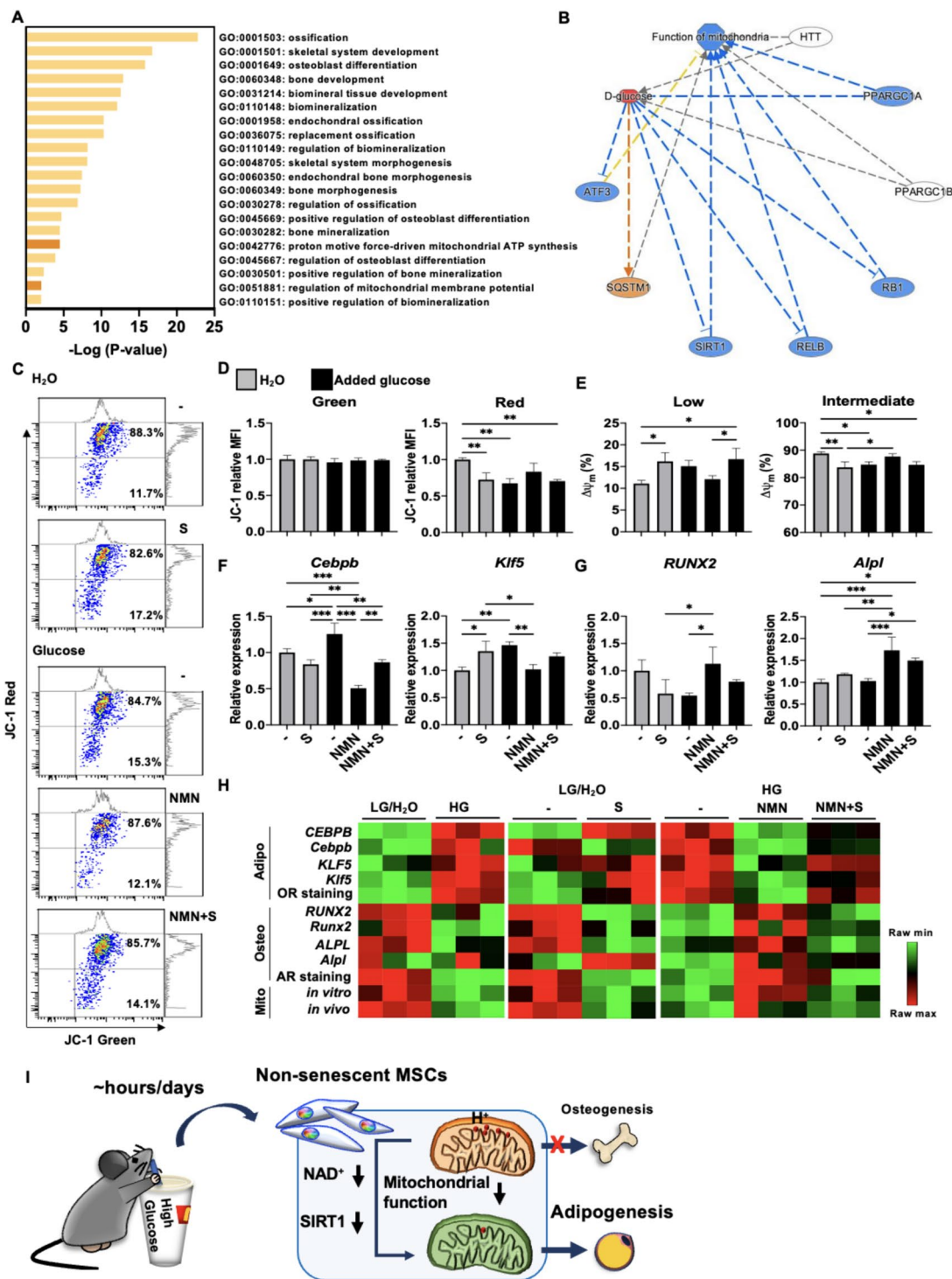
Fig. 6 (See legend on previous page.)

To functionally validate the role of SIRT1 and NAD$^+$ in HG-downregulated mitochondrial metabolism and MSC osteogenesis in vivo, we fed wildtype young adult mice drinking water with additional glucose and assessed the mitochondrial function as well as lineage-specific genes for adipogenesis and osteogenesis in uncultured CD45$^-$ BM cells which contain the MSC population [61, 62]. Acutely, blood glucose levels were significantly increased

in mice receiving glucose-supplemented drinking water compared to those receiving normal water at 4 h. However, the blood glucose levels were similar between the two groups on days 2 and 6 (Figure S4A). These results are in line with previous studies which show that in normal mice, glucose intake rapidly elevates blood glucose levels within hours but can be restored to normal levels thereafter [63, 64]. We found that CD45$^-$ BM cells isolated from mice after 1 day or 5 days of HG intake lost mitochondrial $\Delta\Psi$m. significantly (Figs. 6C, D & S4B-C); and frequencies of mitochondria with low $\Delta\Psi$m. were significantly increased whereas mitochondria with intermediate $\Delta\Psi$m. was significantly decreased at both time points as well (Figs. 6E & S4D-E). In mice drinking normal water, SIRT1 inhibition for 1 day significantly decreased the intensity of mitochondrial $\Delta\Psi$m. as well as frequency of mitochondria with intermediate $\Delta\Psi$m., while significantly increasing mitochondria with low $\Delta\Psi$m. in CD45$^-$ BM cells. Conversely, in mice drinking HG-water, NMN supplementation for 1 day increased the frequency of mitochondria with intermediate $\Delta\Psi$m. in CD45$^-$ BM cells which could be significantly reversed with SIRT1 inhibition; however, at day 5 NMN supplementation did not alter mitochondrial function regardless of whether additional glucose was given or not (Figures S4F-G). Interestingly, lineage commitment towards adipogenesis and away from osteogenesis occurred rapidly after 1 day of HG intake, with significantly upregulated levels of *Cebpb* in CD45$^-$ BM cells regardless of whether NAD$^+$ or SIRT1 was modulated (Figures S4H-I); no changes in levels of osteogenic genes were seen. But by 5 days of HG intake, *Runx2* expression was significantly downregulated, and both *Cebpb* and *Klf5* were upregulated in CD45$^-$ BM cells; moreover, at this time point, NMN supplementation during HG intake significantly decreased both *Cebpb* and *Klf5* while increasing *Runx2* and *Alpl* expression (Figs. 6F, G and S4J-M). SIRT1 inhibition at this time point in normal water intake conditions had a mixed effect on both lineages, significantly decreasing *Cebpb* levels but significantly increasing *Klf5* levels, while decreasing *Runx2* levels and minimally affecting *Alpl*; however, SIRT1 inhibition under NMN supplemented-HG conditions increased levels of *Cebpb* and *Klf5* while decreasing levels of *Runx2* and *Alpl* compared to NMN supplementation alone. These findings demonstrate that while NAD$^+$ depletion due to HG intake can be strongly reversed with oral NMN supplementation, SIRT1 activity is required. Interestingly, the mitochondrial $\Delta\Psi$m. decline seen with HG intake for 1 day can be restored after reversion to regular water for 5 days, but the lineage commitment shift towards adipogenesis/away from osteogenesis could not be restored (Figure S5), implicating the tremendous insult that HG has on MSC osteogenesis.

Moreover, HG intake could have consequences even for end-differentiated adipocytes and osteoblasts; when we lengthened the experiment out to 3-week's time, we found that marrow adipocytes [65, 66] were significantly increased while marrow osteoblasts [67, 68] were significantly decreased in mice drinking HG- vs. regular water (Figure S6). These findings implicate that longer term HG intake may have consequences on more end-differentiated adipocytes and osteoblasts as well. To visually summarize all assessed assays, we utilized heatmap analysis to demonstrate the clear shift in MSC differentiation potential from osteogenesis to adipogenesis as well as mitochondrial functional decline under HG treatment whether in in vitro human or mouse, or in vivo mouse systems (Fig. 6H). Interestingly, there are only 2 discrepant trends seen in the gene expression data of murine *Cebpb* and *Alpl* mainly under normal/LG conditions; both genes are known to involved in the regulation of other stem cell compartments and processes [69–71], which was evident in the in vivo/murine setting of evaluating an entire organ/tissue but not the in vitro/human setting of evaluating only MSCs. Overall, these results demonstrate that in vivo HG intake rapidly downregulates MSC compartment mitochondrial activity as well as strongly modulates lineage commitment towards adipogenesis via the NAD$^+$/SIRT1 axis within 1 to 5 days, with rescue of both mitochondrial activity and osteogenesis possible using oral NMN supplementation which is dependent on SIRT1 activity. Our study provide evidence that HG alone is enough to detrimentally alter young, non-senescent MSC mitochondrial function and osteogenesis to favor adipogenesis within hours in vitro and days in vivo through NAD$^+$ depletion and SIRT1 activity (Fig. 6I).

Discussion

Because over 90% of bone mass is acquired by late adolescence/early adulthood, interventions to significantly improve bone health and decrease OP risk would have the most impact when implemented in these youthful populations [20–22]. Our findings have strong translational implications since we found HG alone-mediated skewing of differentiation from osteogenesis to adipogenesis occurring in non-senescent MSCs in vitro and young mice in vivo. The gain of adipogenic commitment capacity at the expense of osteogenesis in senescent human MSCs is well documented, both in chronological as well as replicative senescence [13, 15–18]. The decreased osteogenesis in aged BM and MSCs has been attributed to decreased SIRT1 levels and/or activity—largely due to senescence-related increased oxidative stress [72, 73] and lower NAD$^+$ levels [37, 38]. In contrast to these studies, we found that even in young, non-senescent MSCs,

Yen *et al. Journal of Biomedical Science*   (2024) 31:49

Page 13 of 17

HG-mediated NAD^+ depletion depressed mitochondrial and SIRT1 function to increase MSC adipogenic commitment at the expense of osteogenic commitment in both in vitro and in vivo settings. Moreover, our data implicates that while the NAD^+ depletion and subsequent detrimental impact on osteogenic commitment caused by a shorter duration of HG conditions (less than 7 days: Figs. 5A-F and 6C-G) can be readily reversed with NMN supplementation, long-term HG conditions (more than 7 days: Figs. 2C, D, 5I, J, S5, and S6) may have a more profound adverse effect on MSC osteogenesis, which has been overwhelmingly found to be more fragile than adipogenesis [74, 75]. Our current data may offer an explanation with regards to the low bone mass seen in teenagers and young adults with the highest intake of simple sugars [24, 26]. Modifiable factors to enhance bone mass are few, with dietary habits being one of such few factors, but while excessive simple sugar intake is well known to increase cardiometabolic disease burden, its link to bone health has not been consistently demonstrated. We found MSCs to express insulin-independent transporters similar to their progeny the osteoblast [30], implicating that MSCs can respond directly to surrounding glucose levels. Our findings may help clarify the correlation of ever higher simple sugar consumption globally in younger and younger age groups [76, 77] to the trend of low bone mass in this age group [21, 22]. Disturbingly, our findings here suggest a possible "double blow" of simple sugar overconsumption on bone health in non-aged, more youthful stages of life—e.g. during adolescence/early adulthood—by directly decreasing the osteogenic capacity of MSCs at the only window of time when peak bone mass can be acquired.

Our report further contributes to the well-documented pro-osteogenic activity of SIRT1 [78, 79]. Through its deacetylase activity and also as a co-factor to a number of developmentally important transcription factors including β-catenin and Foxo3a, we and others have demonstrated that SIRT1 promotes osteogenesis in MSCs and osteoprogenitors by directing increasing expression of RUNX2 and downstream genes including ALPL [35, 36, 80]. More recently, SIRT1-mediated deacetylation of RUNX2 was found to enhance its transcriptional activity [81]. Additionally, likely consequent to the often observed inverse relationship between osteogenesis and adipogenesis, SIRT1 also has been shown to decrease functional MSC adipogenesis [82] as well as *CEBPB* [83] and *KLF5* expression [36]. Collectively, our current findings and these previous reports show that SIRT1 agonism, including via NAD supplementation, strongly shifts MSC lineage commitment towards osteogenesis and away from adipogenesis.

The rapidity and singularity of HG alone in adversely modulating both MSC mitochondrial function and lineage commitment across tissue sources and species of MSCs without the need for lineage-inducing environments was impressive. We found the single molecular crux modulating these functional outcomes to be NAD^+, a molecule central to mitochondrial activity as well as SIRT1 function which modulates the osteogenic transcriptional program through Runx2, the master transcription factor for osteogenesis [35, 84]. When glucose is the predominant substrate, glycolysis is favored over mitochondrial oxidative phosphorylation with consequent depletion of NAD^+, which in turn alters the $NAD^+/NADH$ ratio [32, 85]. This resultant sub-optimal $NAD^+/NADH$ ratio not only compromises mitochondrial oxidative phosphorylation efficiency and mitochondrial membrane potential, but may even lead to cell death [85]. HG can also have direct detrimental effects on mitochondrial function and membrane potential by promoting mitochondrial fission and fragmentation, leading to impaired mitochondrial function and decreased membrane potential ultimately reducing ATP production [86], as well as activating stress signaling pathways such as the NF-κB pathway to contribute to mitochondrial damage [87]. While known for providing energy needed for cell growth and proliferation, the mitochondria within stem cells is increasingly found to be involved in determining cell fate; however, its role in MSC lineage commitment has been less explored [88]. Moreover, while perturbations—including those caused by dietary changes—to NAD^+ levels clearly affect mitochondrial function [89, 90], these important energetics and metabolic aspect of this axis have surprisingly been little explored in MSC biology, with an early study reported mitochondrial membrane potential increasing in in vitro cultured osteoblasts during differentiation into a more mature phenotype [91], and a recent study showed stronger mitochondrial activity in non-senescent MSCs [92]. As complex as mitochondrial molecular mechanisms and functions are, the fact that our findings converge on NAD^+, a single molecule highly sensitive to metabolic changes, helps to explain the rapidity of functional outcomes as well as broad effects of HG alone on both MSC mitochondrial function and lineage commitment. Indeed, the reversal of NAD^+ depletion and its adverse consequences with NMN supplementation also was broad and rapid, occurring within hours/days. Our data strongly implicate that in MSCs, the two functional events of lineage commitment and mitochondrial function are inextricably linked, with stronger mitochondrial function linked to osteogenic commitment controlled by NAD^+ levels.

Encouragingly, we found that NAD^+ depletion due to HG intake can be rapidly reversed with NMN supplementation in these youthful/non-senescent systems in a SIRT1-dependent fashion, reversing MSC adipogenic commitment back towards osteogenesis and improving mitochondrial function as well. NAD^+ biology and supplementation have increasingly been considered to be at the center of numerous age-related functional decline and pathologies, with improving mitochondrial function a commonality in these various aging and disease processes [51]. The ability of NMN supplementation to reverse the anti-osteogenic/pro-adipogenic effects of HG intake also provides an additional weapon with fewer adverse effects and possibly better compliance in the armamentarium against OP and poor bone health. Interestingly, in the in vivo model, adipogenic genes were upregulated more rapidly than osteogenic genes perhaps reflecting the well-known in vitro time course of MSC adipogenesis being much more rapid and achieved in days compared to osteogenesis, which can require up to several weeks [39, 40]. Nevertheless, the overall rapid trend of pro-adipogenic/anti-osteogenic impact of HG intake was seen in vivo as well, with NMN supplementation also able to reverse these changes also within days. The rapidity of NMN-mediated functional reversal in our study is likely due to the youthful/non-senescent MSCs and mice we tested, since recent studies in aged mice demonstrate the need for several weeks to months of supplementation for reversal to occur [90, 93].

Conclusion

Our findings are the first to demonstrate the significant and detrimental impact of a single dietary factor alone on MSC osteogenic capacity in youthful settings. Given the few anabolic therapeutic options, the outsize contribution of OP to global disease disability, and that 90% of peak bone mass is acquired by late adolescence/early adulthood, our data strongly implicate that excessive simple sugar consumption in youthful populations may have far-reaching consequences on bone health. This study also demonstrates NAD^+ not only as the crucial molecule linking HG intake to both MSC mitochondrial activity and osteogenic commitment in non-senescent settings, but also as a probable therapeutic target for improving bone health irrespective of age in our current global environment of sugar overconsumption.

Supplementary Information

The online version contains supplementary material available at https://doi.org/10.1186/s12929-024-01039-0.

Supplementary Material 1.

Availability of data and materials
The microarray datasets used in this study can be accessed at NCBI-GEO: GSE20631 (https://www.ncbi.nlm.nih.gov/geo/query/acc.cgi?acc=GSE20631), GSE45169 (https://www.ncbi.nlm.nih.gov/geo/query/acc.cgi?acc=GSE45169), GSE101140 (https://www.ncbi.nlm.nih.gov/geo/query/acc.cgi?acc=GSE101140), and GSE128423 (https://www.ncbi.nlm.nih.gov/geo/query/acc.cgi?acc=GSE128423).

Declarations

Ethics approval and consent to participate
The animal protocol was approved by the Institutional Animal Care and Use Committee of the NTU (No. 20170426). The isolation of placenta-derived MSCs was conducted after obtaining informed consent of healthy donors approved by the Institutional Review Board of the NTU Hospital.

Consent for publication
Not applicable.

Competing interests
The authors declare that they have no competing financial interests.

Author details
[1]Regenerative Medicine Research Group, Institute of Cellular & System Medicine, National Health Research Institutes (NHRI), No.35, Keyan Road, Zhunan 35053, Taiwan. [2]Department of Obstetrics & Gynecology, National Taiwan University (NTU) Hospital & College of Medicine, NTU, No.1, Section 1, Jen-Ai Road, Taipei 10051, Taiwan. [3]School of Medical Laboratory Science and Biotechnology, College of Medical Science and Technology, Taipei Medical University, No. 250, Wuxing Street, Taipei 11042, Taiwan. [4]Ph.D. Program in Medical Biotechnology, College of Medical Science and Technology, Taipei Medical University, No.250, Wuxing Street, Taipei 11042, Taiwan. [5]Graduate Institute of Life Sciences, National Defense Medical Center (NDMC), No.161, Section 6, Minquan East Road, Taipei 11490, Taiwan. [6]National Institute of Infectious Diseases & Vaccinology, NHRI, No.35, Keyan Road, Zhunan 35053, Taiwan. [7]Graduate Institute of Microbiology & Immunology, NDMC, No.161, Section 6, Minquan East Road, Taipei 11490, Taiwan.

References
1. Meier T, Deumelandt P, Christen O, Stangl GI, Riedel K, Langer M. Global burden of sugar-related dental diseases in 168 countries and corresponding health care costs. J Dent Res. 2017;96:845–54.
2. National Health Promotion Survey (NHIS), https://www.hpa.gov.tw/EngPages/Detail.aspx?nodeid=1077&pid=6201. Health Promotion Administration, Ministry of Health & Welfare, Taiwan.

3. Laguna JC, Alegret M, Cofan M, Sanchez-Tainta A, Diaz-Lopez A, Martinez-Gonzalez MA, Sorli JV, Salas-Salvado J, Fito M, Alonso-Gomez AM, et al. Simple sugar intake and cancer incidence, cancer mortality and all-cause mortality: a cohort study from the PREDIMED trial. Clin Nutr. 2021;40:5269–77.

4. Debras C, Chazelas E, Srour B, Kesse-Guyot E, Julia C, Zelek L, Agaesse C, Druesne-Pecollo N, Galan P, Hercberg S, et al. Total and added sugar intakes, sugar types, and cancer risk: results from the prospective NutriNet-Sante cohort. Am J Clin Nutr. 2020;112:1267–79.

5. Crane PK, Walker R, Hubbard RA, Li G, Nathan DM, Zheng H, Haneuse S, Craft S, Montine TJ, Kahn SE, et al. Glucose levels and risk of dementia. N Engl J Med. 2013;369:540–8.

6. Qi Q, Chu AY, Kang JH, Jensen MK, Curhan GC, Pasquale LR, Ridker PM, Hunter DJ, Willett WC, Rimm EB, et al. Sugar-sweetened beverages and genetic risk of obesity. N Engl J Med. 2012;367:1387–96.

7. Malik VS, Li Y, Pan A, De Koning L, Schernhammer E, Willett WC, Hu FB. Long-term consumption of sugar-sweetened and artificially sweetened beverages and risk of mortality in US adults. Circulation. 2019;139:2113–25.

8. Reid IR. A broader strategy for osteoporosis interventions. Nat Rev Endocrinol. 2020;16:333–9.

9. Wu AM, Bisignano C, James SL, Abady GG, Abedi A, Abu-Gharbieh E, Alhassan RK, Alipour V, Arabloo J, Asaad M, Asmare WN, et al. Global, regional, and national burden of bone fractures in 204 countries and territories, 1990–2019: a systematic analysis from the Global Burden of Disease Study 2019. Lancet Healthy Longev. 2021;2:e580-92.

10. Clynes MA, Harvey NC, Curtis EM, Fuggle NR, Dennison EM, Cooper C. The epidemiology of osteoporosis. Br Med Bull. 2020;133:105–17.

11. Redlich K, Smolen JS. Inflammatory bone loss: pathogenesis and therapeutic intervention. Nat Rev Drug Discov. 2012;11:234–50.

12. Pittenger MF, Discher DE, Peault BM, Phinney DG, Hare JM, Caplan AI. Mesenchymal stem cell perspective: cell biology to clinical progress. NPJ Regen Med. 2019;4:22.

13. Zhou S, Greenberger JS, Epperly MW, Goff JP, Adler C, Leboff MS, Glowacki J. Age-related intrinsic changes in human bone-marrow-derived mesenchymal stem cells and their differentiation to osteoblasts. Aging Cell. 2008;7:335–43.

14. Gimble JM, Zvonic S, Floyd ZE, Kassem M, Nuttall ME. Playing with bone and fat. J Cell Biochem. 2006;98:251–66.

15. Ho PJ, Yen ML, Tang BC, Chen CT, Yen BL. H2O2 accumulation mediates differentiation capacity alteration, but not proliferative decline, in senescent human fetal mesenchymal stem cells. Antioxid Redox Signal. 2013;18:1895–905.

16. D'Ippolito G, Schiller PC, Ricordi C, Roos BA, Howard GA. Age-related osteogenic potential of mesenchymal stromal stem cells from human vertebral bone marrow. J Bone Miner Res. 1999;14:1115–22.

17. Beresford JN, Bennett JH, Devlin C, Leboy PS, Owen ME. Evidence for an inverse relationship between the differentiation of adipocytic and osteogenic cells in rat marrow stromal cell cultures. J Cell Sci. 1992;102(Pt 2):341–51.

18. Nishikawa K, Nakashima T, Takeda S, Isogai M, Hamada M, Kimura A, Kodama T, Yamaguchi A, Owen MJ, Takahashi S, et al. Maf promotes osteoblast differentiation in mice by mediating the age-related switch in mesenchymal cell differentiation. J Clin Invest. 2010;120:3455–65.

19. Compston JE, McClung MR, Leslie WD. Osteoporosis. Lancet. 2019;393:364–76.

20. Henry YM, Fatayerji D, Eastell R. Attainment of peak bone mass at the lumbar spine, femoral neck and radius in men and women: relative contributions of bone size and volumetric bone mineral density. Osteoporos Int. 2004;15:263–73.

21. Berger C, Goltzman D, Langsetmo L, Joseph L, Jackson S, Kreiger N, Tenenhouse A, Davison KS, Josse RG, Prior JC, et al. Peak bone mass from longitudinal data: implications for the prevalence, pathophysiology, and diagnosis of osteoporosis. J Bone Miner Res. 2010;25:1948–57.

22. Hendrickx G, Boudin E, Van Hul W. A look behind the scenes: the risk and pathogenesis of primary osteoporosis. Nat Rev Rheumatol. 2015;11:462–74.

23. Chevalley T, Rizzoli R. Acquisition of peak bone mass. Best Pract Res Clin Endocrinol Metab. 2022;36:101616.

24. Wyshak G. Teenaged girls, carbonated beverage consumption, and bone fractures. Arch Pediatr Adolesc Med. 2000;154:610–3.

25. Gender statistics data, https://www.mohw.gov.tw/dl-13424-64eb6290-6a45-4a5d-aa6a-77b5c3deb327.html. Ministry of Health & Welfare, Taiwan.

26. Marriott BP, Cole N, Lee E. National estimates of dietary fructose intake increased from 1977 to 2004 in the United States. J Nutr. 2009;139:1228S-1235S.

27. Cao B, Liu N, Wang W. High glucose prevents osteogenic differentiation of mesenchymal stem cells via lncRNA AK028326/CXCL13 pathway. Biomed Pharmacother. 2016;84:544–51.

28. Morganti C, Missiroli S, Lebiedzinska-Arciszewska M, Ferroni L, Morganti L, Perrone M, Ramaccini D, Occhionorelli S, Zavan B, Wieckowski MR, et al. Regulation of PKCbeta levels and autophagy by PML is essential for high-glucose-dependent mesenchymal stem cell adipogenesis. Int J Obes (Lond). 2019;43:963–73.

29. Li YM, Schilling T, Benisch P, Zeck S, Meissner-Weigl J, Schneider D, Limbert C, Seufert J, Kassem M, Schutze N, et al. Effects of high glucose on mesenchymal stem cell proliferation and differentiation. Biochem Biophys Res Commun. 2007;363:209–15.

30. Wei J, Shimazu J, Makinistoglu MP, Maurizi A, Kajimura D, Zong H, Takarada T, Lezaki T, Pessin JE, Hinoi E, et al. Glucose Uptake and Runx2 Synergize to Orchestrate Osteoblast Differentiation and Bone Formation. Cell. 2015;161:1576–91.

31. Chini CCS, Zeidler JD, Kashyap S, Warner G, Chini EN. Evolving concepts in NAD(+) metabolism. Cell Metab. 2021;33:1076–87.

32. Ryall JG, Dell'Orso S, Derfoul A, Juan A, Zare H, Feng X, Clermont D, Koulnis M, Gutierrez-Cruz G, Fulco M, et al. The NAD(+)-dependent SIRT1 deacetylase translates a metabolic switch into regulatory epigenetics in skeletal muscle stem cells. Cell Stem Cell. 2015;16:171–83.

33. Bonkowski MS, Sinclair DA. Slowing ageing by design: the rise of NAD(+) and sirtuin-activating compounds. Nat Rev Mol Cell Biol. 2016;17:679–90.

34. Wang CH, Wei YH. Roles of Mitochondrial Sirtuins in Mitochondrial Function, Redox Homeostasis, Insulin Resistance and Type 2 Diabetes. Int J Mol Sci. 2020;21:5266.

35. Tseng PC, Hou SM, Chen RJ, Peng HW, Hsieh CF, Kuo ML, Yen ML. Resveratrol promotes osteogenesis of human mesenchymal stem cells by upregulating RUNX2 gene expression via the SIRT1/FOXO3A axis. J Bone Miner Res. 2011;26:2552–63.

36. Lin CH, Li NT, Cheng HS, Yen ML. Oxidative stress induces imbalance of adipogenic/osteoblastic lineage commitment in mesenchymal stem cells through decreasing SIRT1 functions. J Cell Mol Med. 2018;22:786–96.

37. Li Y, He X, Li Y, He J, Anderstam B, Andersson G, Lindgren U. Nicotinamide phosphoribosyltransferase (Nampt) affects the lineage fate determination of mesenchymal stem cells: a possible cause for reduced osteogenesis and increased adipogenesis in older individuals. J Bone Miner Res. 2011;26:2656–64.

38. Kim HN, Ponte F, Warren A, Ring R, Iyer S, Han L, Almeida M. A decrease in NAD(+) contributes to the loss of osteoprogenitors and bone mass with aging. NPJ Aging Mech Dis. 2021;7:8.

39. Yen BL, Huang HI, Chien CC, Jui HY, Ko BS, Yao M, Shun CT, Yen ML, Lee MC, Chen YC. Isolation of multipotent cells from human term placenta. Stem Cells. 2005;23:3–9.

40. Pittenger MF, Mackay AM, Beck SC, Jaiswal RK, Douglas R, Mosca JD, Moorman MA, Simonetti DW, Craig S, Marshak DR. Multilineage potential of adult human mesenchymal stem cells. Science. 1999;284:143–7.

41. Wang LT, Wang HH, Chiang HC, Huang LY, Chiu SK, Siu LK, Liu KJ, Yen ML, Yen BL. Human Placental MSC-Secreted IL-1beta Enhances Neutrophil Bactericidal Functions during Hypervirulent Klebsiella Infection. Cell Rep. 2020;32:108188.

42. Lee W, Wang LT, Yen ML, Hsu PJ, Lee YW, Liu KJ, Lin KI, Su YW, Sytwu HK, Yen BL. Resident vs nonresident multipotent mesenchymal stromal cell interactions with B lymphocytes result in disparate outcomes. Stem Cells Transl Med. 2021;10:711–24.

43. Wang LT, Lee YW, Bai CH, Chiang HC, Wang HH, Yen BL, Yen ML. A Rapid and Highly Predictive in vitro Screening Platform for Osteogenic Natural Compounds Using Human Runx2 Transcriptional Activity in Mesenchymal Stem Cells. Front Cell Dev Biol. 2021;8:607383.

44. Baryawno N, Przybylski D, Kowalczyk MS, Kfoury Y, Severe N, Gustafsson K, Kokkaliaris KD, Mercier F, Tabaka M, Hofree M, et al. A Cellular taxonomy of the bone marrow stroma in homeostasis and leukemia. Cell. 2019;177:1915-1932 e16.

Yen *et al. Journal of Biomedical Science*   (2024) 31:49

Page 16 of 17

45. Zhou Y, Zhou B, Pache L, Chang M, Khodabakhshi AH, Tanaseichuk O, Benner C, Chanda SK. Metascape provides a biologist-oriented resource for the analysis of systems-level datasets. Nat Commun. 2019;10:1523.

46. Wang LT, Yen BL, Wang HH, Chao YY, Lee W, Huang LY, Chiu SK, Siu LK, Liu KJ, Sytwu HK, Yen ML. Placental mesenchymal stem cells boost M2 alveolar over M1 bone marrow macrophages via IL-1beta in Klebsiella-mediated acute respiratory distress syndrome. Thorax. 2023;78:504–14.

47. Sakamuri S, Sperling JA, Sure VN, Dholakia MH, Peterson NR, Rutkai I, Mahalingam PS, Satou R, Katakam PVG. Measurement of respiratory function in isolated cardiac mitochondria using Seahorse XFe24 Analyzer: applications for aging research. Geroscience. 2018;40:347–56.

48. Cheng CW, Biton M, Haber AL, Gunduz N, Eng G, Gaynor LT, Tripathi S, Calibasi-Kocal G, Rickelt S, Butty VL, et al. Ketone Body Signaling Mediates Intestinal Stem Cell Homeostasis and Adaptation to Diet. Cell. 2019;178:1115-1131 e15.

49. Bertoldo MJ, Listijono DR, Ho WJ, Riepsamen AH, Goss DM, Richani D, Jin XL, Mahbub S, Campbell JM, Habibalahi A, et al. NAD(+) repletion rescues female fertility during reproductive aging. Cell Rep. 2020;30:1670-1681 e7.

50. Ye Q, Zhang M, Wang Y, Fu S, Han S, Wang L, Wang Q. Sirtinol regulates the balance of Th17/Treg to prevent allograft rejection. Cell Biosci. 2017;7:55.

51. Yoshino J, Baur JA, Imai SI. NAD(+) Intermediates: the biology and therapeutic potential of NMN and NR. Cell Metab. 2018;27:513–28.

52. Gohil VM, Sheth SA, Nilsson R, Wojtovich AP, Lee JH, Perocchi F, Chen W, Clish CB, Ayata C, Brookes PS, et al. Nutrient-sensitized screening for drugs that shift energy metabolism from mitochondrial respiration to glycolysis. Nat Biotechnol. 2010;28:249–55.

53. Sharpe PC, Yue KK, Catherwood MA, McMaster D, Trimble ER. The effects of glucose-induced oxidative stress on growth and extracellular matrix gene expression of vascular smooth muscle cells. Diabetologia. 1998;41:1210–9.

54. Lee EA, Seo JY, Jiang Z, Yu MR, Kwon MK, Ha H, Lee HB. Reactive oxygen species mediate high glucose-induced plasminogen activator inhibitor-1 up-regulation in mesangial cells and in diabetic kidney. Kidney Int. 2005;67:1762–71.

55. Askwith T, Zeng W, Eggo MC, Stevens MJ. Oxidative stress and dysregulation of the taurine transporter in high-glucose-exposed human Schwann cells: implications for pathogenesis of diabetic neuropathy. Am J Physiol Endocrinol Metab. 2009;297:E620–8.

56. Zheng CX, Sui BD, Qiu XY, Hu CH, Jin Y. Mitochondrial Regulation of Stem Cells in Bone Homeostasis. Trends Mol Med. 2020;26:89–104.

57. de Picciotto NE, Gano LB, Johnson LC, Martens CR, Sindler AL, Mills KF, Imai S, Seals DR. Nicotinamide mononucleotide supplementation reverses vascular dysfunction and oxidative stress with aging in mice. Aging Cell. 2016;15:522–30.

58. Mitchell SJ, Bernier M, Aon MA, Cortassa S, Kim EY, Fang EF, Palacios HH, Ali A, Navas-Enamorado I, Di Francesco A, et al. Nicotinamide improves aspects of Healthspan, but not lifespan, in mice. Cell Metab. 2018;27:667-676 e4.

59. Gao Z, Zhang J, Kheterpal I, Kennedy N, Davis RJ, Ye J. Sirtuin 1 (SIRT1) protein degradation in response to persistent c-Jun N-terminal kinase 1 (JNK1) activation contributes to hepatic steatosis in obesity. J Biol Chem. 2011;286:22227–34.

60. Yao Z, Yang W, Gao Z, Jia P. Nicotinamide mononucleotide inhibits JNK activation to reverse Alzheimer disease. Neurosci Lett. 2017;647:133–40.

61. Severe N, Karabacak NM, Gustafsson K, Baryawno N, Courties G, Kfoury Y, Kokkaliaris KD, Rhee C, Lee D, Scadden EW, et al. Stress-induced changes in bone marrow stromal cell populations revealed through single-cell protein expression mapping. Cell Stem Cell. 2019;25:570-583 e7.

62. Baccin C, Al-Sabah J, Velten L, Helbling PM, Grunschlager F, Hernandez-Malmierca P, Nombela-Arrieta C, Steinmetz LM, Trumpp A, Haas S. Combined single-cell and spatial transcriptomics reveal the molecular, cellular and spatial bone marrow niche organization. Nat Cell Biol. 2020;22:38–48.

63 Furman BL. Streptozotocin-Induced Diabetic Models in Mice and Rats. Curr Protoc Pharmacol. 2015;70:5 47 1-5 47 20.

64. Zhan X, Wang L, Wang Z, Chai S, Zhu X, Ren W, Chang X. High-glucose administration induces glucose intolerance in mice: a critical role of toll-like receptor 4. J Clin Biochem Nutr. 2019;64:194–200.

65. Christiaens V, Van Hul M, Lijnen HR, Scroyen I. CD36 promotes adipocyte differentiation and adipogenesis. Biochim Biophys Acta. 2012;1820:949–56.

66. Miggitsch C, Meryk A, Naismith E, Pangrazzi L, Ejaz A, Jenewein B, Wagner S, Nagele F, Fenkart G, Trieb K, et al. Human bone marrow adipocytes display distinct immune regulatory properties. EBioMedicine. 2019;46:387–98.

67. Nguyen TM, Arthur A, Panagopoulos R, Paton S, Hayball JD, Zannettino AC, Purton LE, Matsuo K, Gronthos S. EphB4 expressing stromal cells exhibit an enhanced capacity for hematopoietic stem cell maintenance. Stem Cells. 2015;33:2838–49.

68. Arthur A, Nguyen TM, Paton S, Zannettino ACW, Gronthos S. Loss of EfnB1 in the osteogenic lineage compromises their capacity to support hematopoietic stem/progenitor cell maintenance. Exp Hematol. 2019;69:43–53.

69. Martin GR, Evans MJ. Differentiation of clonal lines of teratocarcinoma cells: formation of embryoid bodies in vitro. Proc Natl Acad Sci U S A. 1975;72:1441–5.

70. Ali AT, Penny CB, Paiker JE, van Niekerk C, Smit A, Ferris WF, Crowther NJ. Alkaline phosphatase is involved in the control of adipogenesis in the murine preadipocyte cell line, 3T3-L1. Clin Chim Acta. 2005;354:101–9.

71. Sato A, Kamio N, Yokota A, Hayashi Y, Tamura A, Miura Y, Maekawa T, Hirai H. C/EBPbeta isoforms sequentially regulate regenerating mouse hematopoietic stem/progenitor cells. Blood Adv. 2020;4:3343–56.

72. Simic P, Zainabadi K, Bell E, Sykes DB, Saez B, Lotinun S, Baron R, Scadden D, Schipani E, Guarente L. SIRT1 regulates differentiation of mesenchymal stem cells by deacetylating beta-catenin. EMBO Mol Med. 2013;5:430–40.

73. Ucer S, Iyer S, Kim HN, Han L, Rutlen C, Allison K, Thostenson JD, de Cabo R, Jilka RL, O'Brien C, et al. The effects of aging and sex steroid deficiency on the murine skeleton are independent and mechanistically distinct. J Bone Miner Res. 2017;32:560–74.

74. Pierce JL, Begun DL, Westendorf JJ, McGee-Lawrence ME. Defining osteoblast and adipocyte lineages in the bone marrow. Bone. 2019;118:2–7.

75. Hart DA. Is adipocyte differentiation the default lineage for mesenchymal stem/progenitor cells after loss of mechanical loading? A perspective from space flight and model systems. J Biomed Sci Eng. 2014;7:799–808.

76. Vos MB, Kaar JL, Welsh JA, Van Horn LV, Feig DI, Anderson CAM, Patel MJ, Cruz Munos J, Krebs NF, Xanthakos SA, et al. Added sugars and cardiovascular disease risk in children: a scientific statement from the american heart association. Circulation. 2017;135:e1017–34.

77. Guideline: Sugars Intake for Adults and Children. WHO Guidelines Approved by the Guidelines Review Committee. 2015.

78. Kim HN, Iyer S, Ring R, Almeida M. The role of FoxOs in bone health and disease. Curr Top Dev Biol. 2018;127:149–63.

79. Chen Y, Zhou F, Liu H, Li J, Che H, Shen J, Luo E. SIRT1, a promising regulator of bone homeostasis. Life Sci. 2021;269:119041.

80. Iyer S, Han L, Bartell SM, Kim HN, Gubrij I, de Cabo R, O'Brien CA, Manolagas SC, Almeida M. Sirtuin1 (Sirt1) promotes cortical bone formation by preventing beta-catenin sequestration by FoxO transcription factors in osteoblast progenitors. J Biol Chem. 2014;289:24069–78.

81. Louvet L, Leterme D, Delplace S, Miellot F, Marchandise P, Gauthier V, Hardouin P, Chauveau C, Ghali MO. Sirtuin 1 deficiency decreases bone mass and increases bone marrow adiposity in a mouse model of chronic energy deficiency. Bone. 2020;136:115361.

82. Backesjo CM, Li Y, Lindgren U, Haldosen LA. Activation of Sirt1 decreases adipocyte formation during osteoblast differentiation of mesenchymal stem cells. J Bone Miner Res. 2006;21:993–1002.

83. Ding H, Chen J, Qin J, Chen R, Yi Z. TGF-beta-induced alpha-SMA expression is mediated by C/EBPbeta acetylation in human alveolar epithelial cells. Mol Med. 2021;27:22.

84. Ducy P, Schinke T, Karsenty G. The osteoblast: a sophisticated fibroblast under central surveillance. Science. 2000;289:1501–4.

85. Stein LR, Imai S. The dynamic regulation of NAD metabolism in mitochondria. Trends Endocrinol Metab. 2012;23:420–8.

86. Audzeyenka I, Rachubik P, Typiak M, Kulesza T, Topolewska A, Rogacka D, Angielski S, Saleem MA, Piwkowska A. Hyperglycemia alters mitochondrial respiration efficiency and mitophagy in human podocytes. Exp Cell Res. 2021;407:112758.

87. Zhang Z, Huang Q, Zhao D, Lian F, Li X, Qi W. The impact of oxidative stress-induced mitochondrial dysfunction on diabetic microvascular complications. Front Endocrinol (Lausanne). 2023;14:1112363.
88. Chakrabarty RP, Chandel NS. Mitochondria as signaling organelles control mammalian stem cell fate. Cell Stem Cell. 2021;28:394–408.
89. Okabe K, Yaku K, Tobe K, Nakagawa T. Implications of altered NAD metabolism in metabolic disorders. J Biomed Sci. 2019;26:34.
90. Elamin M, Ruskin DN, Sacchetti P, Masino SA. A unifying mechanism of ketogenic diet action: the multiple roles of nicotinamide adenine dinucleotide. Epilepsy Res. 2020;167:106469.
91. Komarova SV, Ataullakhanov FI, Globus RK. Bioenergetics and mitochondrial transmembrane potential during differentiation of cultured osteoblasts. Am J Physiol Cell Physiol. 2000;279:C1220–9.
92. Fernandez-Rebollo E, Franzen J, Goetzke R, Hollmann J, Ostrowska A, Oliverio M, Sieben T, Rath B, Kornfeld JW, Wagner W. Senescence-associated Metabolomic phenotype in primary and ipsc-derived mesenchymal stromal cells. Stem Cell Reports. 2020;14:201–9.
93. Song J, Li J, Yang F, Ning G, Zhen L, Wu L, Zheng Y, Zhang Q, Lin D, Xie C, et al. Nicotinamide mononucleotide promotes osteogenesis and reduces adipogenesis by regulating mesenchymal stromal cells via the SIRT1 pathway in aged bone marrow. Cell Death Dis. 2019;10:336.

Publisher's Note

Springer Nature remains neutral with regard to jurisdictional claims in published maps and institutional affiliations.